JTTEE5 19:1277–1286
DOI: 10.1007/s11666-010-9519-7
1059-9630/$19.00 © ASM International

Review of Thermal Spray Coating Applications in the Steel Industry: Part 2—Zinc Pot Hardware in the Continuous Galvanizing Line

S. Matthews and B. James

(Submitted December 16, 2009; in revised form May 26, 2010)

This two-part article series reviews the application of thermal spray coating technology in the production of steel and steel sheet products. Part 2 of this article series is dedicated to coating solutions in the continuous galvanizing line. The corrosion mechanisms of Fe- and Co-based bulk materials are briefly reviewed as a basis for the development of thermal spray coating solutions. WC-Co thermal spray coatings are commonly applied to low Al-content galvanizing hardware due to their superior corrosion resistance compared to Fe and Co alloys. The effect of phase degradation, carbon content, and WC grain size are discussed. At high Al concentrations, the properties of WC-Co coatings degrade significantly, leading to the application of oxide-based coatings and corrosion-resistant boride containing coatings. The latest results of testing are summarized, highlighting the critical coating parameters.

Keywords advantages of TS, ceramic oxide layers, cermet coatings, coatings for rolls, corrosion, corrosion of HVOF coatings, novel materials

1. Introduction

Steel sheet destined for use outdoors or in potentially corrosive applications is coated to improve its corrosion resistance. This is most commonly achieved using a continuous hot-dip process in which a zinc-based coating is applied to both sides of the steel sheet (Ref 1, 2). The most common zinc-based coatings are:

- *Galvanized zinc*, with an aluminum concentration below 0.3 wt.% (Ref 1-3). This composition has a bath temperature of 445-455 °C (Ref 2).
- *Galfan*, a Zn-5 wt.% Al alloy (Ref 1, 2). This composition is a low melting point eutectic with a typical bath temperature of 425 °C (Ref 2).
- *Galvalume*, a Zn-55 wt.%Al alloy with additions of up to 1.5 wt.% Si (Ref 1, 2, 4). The high melting point of this alloy requires a bath temperature of approximately 600 °C (Ref 1, 2).

S. Matthews, School of Engineering and Advanced Technology, Massey University, Auckland, New Zealand; and **B. James**, Department of Chemical and Materials Engineering, University of Auckland, Auckland, New Zealand. Contact e-mail: s.matthews@massey.ac.nz.

In this process, the continuous, cleaned, and heat-treated steel sheet passes from the annealing line over a turn down roll into the galvanizing pot containing the molten Zn-based metal (Fig. 1). Within the pot the sink (Ref 5) or sinker (Ref 1) roll directs the incoming sheet toward the base of the pot and then changes its direction to head vertically upward out of the pot toward the gas wiping dies (Ref 1, 5). The die geometry, the velocity of gas they eject, and the die to steel sheet distance are critical variables in controlling the thickness and uniformity of the Zn coating (Ref 5). The deflector roll can be moved horizontally to control the tension in the steel sheet (Ref 5) and reduce the curvature in the plane of the sheet (Ref 1). The stationary corrector roll repositions the deflected sheet to align it with the wiping dies (Ref 1). Touch rolls above the wiping dies support the sheet and reduce vibrations which may vary the wiper-sheet spacing (Ref 1).

Corrosion of the submerged pot hardware by the molten Zn alloy significantly reduces their functionality and operating lifetime (Ref 6). Roller bearings have typical operating lifetimes of 6-30 days depending on the operating conditions (Ref 5). Corrosion increases the friction within the bearings which prevents the rolls from turning (Ref 5) and leads to scratching and poor quality steel strip (Ref 7, 8). It can also generate excessive strip vibration which contributes to poor surface quality (Ref 6).

Corrosion of the roll surfaces degrades the surface finish and results in the build-up of dross particles (Ref 7, 8). Dross particles form by the reaction of Zn and Al in the melt with iron and iron oxides from the steel sheet (Ref 2, 7-9) to form ZnO and Al_2O_3 oxides (Ref 2, 9). Iron released in this reaction and from dissolution of the steel

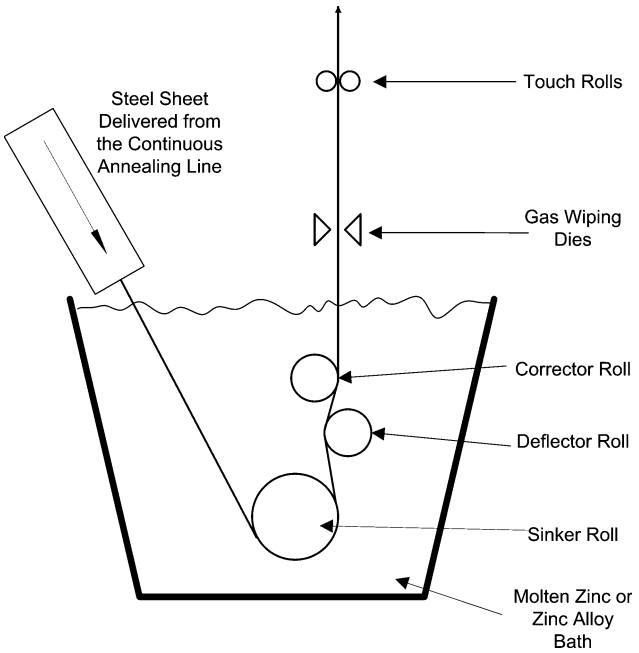

Fig. 1 Schematic diagram of the pot region of a continuous hot-dip metal coating line. Schematic redrawn based on Ref 1 and 4

sheet saturates the Zn melt and leads to the formation of intermetallic compounds. Aluminum-saturated $FeZn_7$ settles out as "bottom dross" (Ref 2), while $Fe_2Al_5Zn_X$ remains suspended or floats as "top dross" (Ref 2). The highest concentration of top dross occurs in the "V" region formed as the steel sheet enters the bath, passes under the sink roll, and then exits the bath (Ref 8, 9). Dissolution of the iron sheet leads to localized bath iron concentrations an order of magnitude higher than the equilibrium iron solubility (Ref 8). This generates high localized concentrations of dross particles which attach and agglomerate on the corrosion products formed on the sink rolls (Ref 8). These particles are harder than steel and generate surface defects in the steel strip (Ref 10) as well as reducing the homogeneity and quality of the Zn alloy coating on the steel surface (Ref 7, 8). Occasionally dross particles break away from the roll and adhere to the steel (Ref 7), further compromising the Zn-coating quality. Most continuous galvanizing lines operate for an average of only 2 weeks before requiring downtime for hardware maintenance and replacement (Ref 7, 11). With a typical turn around time of 3 days to restore normal operation (Ref 7), the effects of corrosion are extremely expensive in terms of hardware replacement and lost production time.

2. Galvanizing Hardware Materials

316L Stainless Steel is the most widely used material for the fabrication of galvanizing pot hardware because of its balance of acceptable corrosion resistance to liquid zinc, at reasonable cost (Ref 8). Stellite 6 is also widely

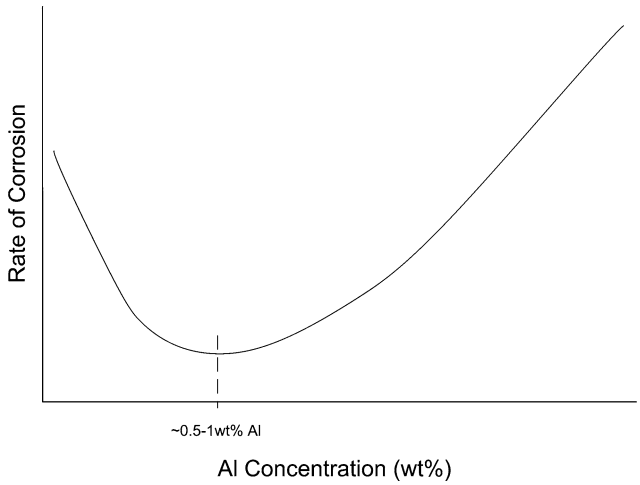

Fig. 2 Schematic diagram of the generic corrosion rate of iron alloys as a function of the bath Al concentration. Schematic redrawn based on Ref 14 and 18

used for sleeve, bearing, and bush materials where greater wear resistance is required (Ref 12-14). The liquid Zn corrosion mechanism of these Fe- and Co-based materials form the background of most proprietary alloy developments. They are discussed here as a basis for the development of thermally sprayed coating compositions in the following sections.

2.1 Iron-Based Alloys

Galvanizing in pure Zn results in the rapid dissolution of Fe (Ref 15). Simultaneously, Zn reacts with the Fe surface to form a continuous layer of intermetallic compounds (e.g., Fe_3Zn_{10}, $FeZn_{10}$, and $FeZn_{13}$) which acts to reduce the Fe dissolution rate (Ref 2, 14). Zinc diffuses through this layer, enabling it to grow into the Fe alloy (Ref 2, 15) at a rate based on the parabolic rate law (Ref 15). As it thickens, the brittle intermetallic undergoes localized spallation, followed by rapid reformation, leading to cumulative mass loss of the alloy (Ref 15). Iron corrosion is therefore dictated by the diffusion of Zn through the intermetallic layer.

The addition of Al to the Zn melt inhibits Fe-Zn intermetallic formation by preferentially reacting with Fe (Ref 2, 8, 14, 16, 17). Additions of up to 0.15 wt.% Al significantly reduces the corrosion rate of Fe alloys (Fig. 2), by reducing the concentration and activity of Zn, thereby reducing the rate of the Fe-Zn reaction and of Zn diffusion through the intermetallic layer (Ref 14). The high affinity of Al for Fe leads to Al segregation at the iron surface where it reacts to form an "inhibition layer" of Fe-Al complexes. This layer significantly reduces the dissolution rate of Fe and inhibits the Fe-Zn reaction rate (Ref 14, 17, 18). However, the mechanisms that dictate the extent of corrosion and mass loss are still based on the Fe-Zn reaction described for pure Zn.

Additions of 0.1-0.3 wt.% Al are added to the galvanizing bath to "inhibit" the formation of the brittle

intermetallic phases on the steel sheet (Ref 1, 2, 14). However, this effect is only temporary on the iron-based bath hardware due to breakdown of the inhibition layer with extended exposure. Zinc diffusion leads to attack of the underlying Fe metal, resulting in ''outbursts'' of Fe-Zn intermetallic material through the inhibition layer (Ref 2).

Above 0.15 wt.%, Al becomes the most corrosive element (Ref 16, 19) and the Al-Fe reaction dominates over the Zn-Fe reaction (Ref 14) to form a thermodynamically stable interface phase of Fe_2Al_5 (Ref 2). Aluminum atoms within this layer diffuse to the steel-Fe_2Al_5 interface where they react and cause the intermetallic phase to grow further into the steel substrate (Ref 8). As this layer thickens, the reaction rate slows according to the parabolic rate law (Ref 8). Concurrently, Fe and alloying elements such as Ni and Cr diffuse through the Fe_2Al_5 layer and are dissipated in the Zn bath (Ref 8, 16). With extended exposure, Zn diffuses into the Fe_2Al_5 layer to occupy vacancies left by Al diffusion and reacts to form $Fe_2Al_5Zn_X$ compounds (Ref 8, 20). These compounds react with ''top dross'' particles of similar composition and accentuate the build-up of dross material on the surface of the bath hardware. With extended exposure, the outer layer of $Fe_2Al_5Zn_X$ begins to break down and dissolve as Zn diffusion causes the equilibrium composition to change (Ref 20). A complex-banded structure forms as a function of the local Zn concentration (Eq 1) (Ref 20).

$$\begin{aligned} Fe_2Al_5 \rightarrow Fe_2Al_5Zn_X \rightarrow \text{Liquid} + Fe_2Al_5Zn_X + FeZn_7 \\ \rightarrow \text{Liquid} + FeZn_7 \rightarrow \text{Liquid Substrate reaction} \\ \text{front} \rightarrow \text{Liquid Zn in bath} \end{aligned} \quad \text{(Eq 1)}$$

At 5 wt.% (''galfan'' composition), the Al-content is high enough to prevent Fe-Zn intermetallic formation for short exposure periods (Ref 2). However, with extended exposure the $Fe_2Al_5Zn_X$ inhibition layer begins to breakdown, with Zn attacking the steel substrate to form Fe-Zn intermetallic ''outbursts'' (Ref 2).

In ''galvalume'' baths containing 55 wt.% Al, Fe alloys are rapidly consumed by the formation of Fe_2Al_5 and $FeAl_3$ (Ref 2). The rapid breakdown and flaking of this reaction layer prevents the formation of a stable inhibition layer (Ref 2). Silicon is added to suppress the Fe-Al reaction by forming a solid diffusion barrier on the steel surface (Ref 1, 2). Corrosion then occurs by diffusion of Al through the silicon boundary layer to the internal reaction front in the steel. Localized breakdown of the Si diffusion barrier results in rapid Fe_2Al_5 and $FeAl_3$ ''outburst'' formation (Ref 2).

Alloying elements in iron and steel lead to minor changes to the generic mechanisms discussed with their primary effect appearing to be their influence on the reaction kinetics (Ref 2, 9). The influence of specific alloying elements has been discussed in detail by Morando (Ref 9) in the development of Zn-Al corrosion-resistant Fe-based alloys, and by Zhang and Tang (Ref 19), Wang et al. (Ref 21), Bright (Ref 13), and Xu et al. (Ref 16) in the testing of Fe-based superalloys.

2.2 Cobalt-Based Alloys

Co-based Stellite® alloys are extensively used for galvanizing hardware (Ref 13, 18, 19, 22, 23) and their reaction and dissolution mechanism closely parallel those of Fe alloys. Aluminum reacts with Co to form a Co-Al surface layer, even at very low Al concentrations (Ref 19). Discrete Co-Al particles form out from the surface as Co diffuses from the substrate into the melt (Ref 19), while Al diffuses through the intermetallic layer to propagate the reaction front further into the alloy. Behind this reaction front, the reaction products react with Zn to form complex Zn-based layers. Flow of the molten Zn-Al bath past these corrosion layers enhances the dissolution of Co from the alloy and accelerates the breakdown and spallation of the reaction layers (Ref 24).

With extended exposure, the Co-Al phase either dissolves into the Zn-Al melt or reacts with Fe dissolved in the melt to form Fe_2Al_5 (Ref 10, 19). As in Fe alloys, top dross Fe_2Al_5 particles in the melt readily agglomerate on the Fe_2Al_5 phases on the alloy surface and build-up to the point where they adversely effect the Zn-coating quality on the steel sheet (Ref 19).

The addition of alloying elements to form carbide or Laves phases improves the Zn-Al corrosion resistance (Ref 13, 19, 23, 24). However, such phases eventually also react with Al, undergoing dissolution or reaction to form other phases (Ref 13, 19). In addition, reaction and dissolution of the surrounding Co matrix leave these phases prone to detachment by the moving Zn-Al melt, accelerating the corrosive attack on the alloy (Ref 24).

3. Thermal Spray Coating Solutions in Continuous Galvanizing Lines

3.1 Tungsten Carbide-Cobalt (WC-Co) Thermal Spray Coatings

3.1.1 Galvanizing Baths (<0.3% Al). WC-(10-15 wt.%)Co thermal spray coatings are commonly applied to galvanizing hardware due to their superior corrosion resistance relative to Fe and Co alloys (Ref 7, 25-31). The success of this cermet relies on generating a degree of reaction between the WC and Co phases (Ref 32) to improve the poor corrosion response of Co in molten Zn. This concept is in direct contrast to that of traditional WC-Co coatings for wear applications where phase reaction is avoided as much as possible (Ref 33-35). Wear applications typically use WC-Co thermal spray powders produced via spray drying, blending, or cladding (Ref 32) routes where WC and pure Co dominate the powder composition. Conversely greater phase interaction occurs in sintered and crushed, cast/fused and crushed and plasma densified powders which form more Zn corrosion-resistant mixed Co-W-C phases (e.g., Co_3W_3C, Co_6W_6C, $W_6C_{2.54}$, and Co_2W_4C) (Ref 32). In contrasting the effect of powder production route, Tomita et al. (Ref 36) observed a 200-μm-thick spray dried based WC-Co Jet Kote HVOF coating to totally

dissolve within 48 h in a Zn bath, while negligible thickness loss occurred on a sintered/crushed powder-based Jet Kote HVOF coating out to 96 h. The high retained Co-content in the spray dried powder-based coating readily dissolved in pure Zn and was replaced by Zn-Co intermetallic compounds. The removal of the coherent binder undermined the WC grains which dropped out of the coating. In contrast, it was postulated that the isolated pockets of pure Co in the sintered/crushed powder-based coating created a tortuous diffusion path for Zn around the corrosion-resistant WC particles and slower reacting Co-W-C phases. It is important to highlight that it is the phase reaction that is significant in this intermetallic effect, not phase decarburisation which can also occur during thermal spraying. Decarburisation can form free W which is less corrosion-resistant than WC to liquid Zn (Ref 32).

Reduction of the WC-Co carbon content can also improve the Zn corrosion resistance by increasing the concentration of Co_3W_3C and Co_6W_6C carbides and decreasing the free Co content (Ref 37, 38). A reduction in the carbon content from 5.5 to 4.2 wt.% in a WC-12 wt.% Co JP-5000 HVOF cermet increased the time to failure in a galvalume bath from 209 to 358 h in the work of Mizuno and Kitamura (Ref 39). In a related trial, the reduction in carbon content was attributed to extending the coating lifetime from 120 to 213 h (Ref 37).

The complex Co-W-C binder composition may also be achieved by manipulating the starting carbide grains size in order to generate carbide dissolution during thermal spray. Jarosinski et al. (Ref 40) observed improved corrosion performance in WC-Co JP-5000 HVOF coatings in Zn-Al baths with decreasing carbide grain size from 1 to 3 μm down to 0.5 to 1 μm for a fixed cermet composition. Finer carbides are more prone to dissolution into the Co binder during thermal spray to form complex Co-W-C phases and consequently reduce the elemental cobalt concentration (Ref 40). The lower limit of the starting carbide size is dictated by the thermal spray deposition technique—the carbide size and deposition parameters must be balanced to achieve the desired degree of Co-W-C formation without excessive carbide dissolution or decarburization which reduce the wear and corrosion resistance of the coating (Ref 41). Presumably, it is this mechanism which accounts for the recent success of superfine WC-Co powder feedstocks in industrial galvanizing lines (Ref 42).

3.1.2 Effect of Higher Al Concentrations. Increasing the Al concentration from 0.3 to 3 wt.% in the Zn bath reduces the corrosion rate of WC-Co cermets with Co-W-C binders by reducing the depth of Zn diffusion into the binder phase (Ref 10, 43, and Fig. 3). Tani et al. (Ref 43) postulate that rapid dissolution of pure Co occurs, while concurrently Zn diffuses into the coating Co binder phase (Fig. 4). It was notable that minimal Al diffusion into the Co binder occurred in their work. The dissolved Co reacts with the bath elements to form Co-Al and Co-Zn intermetallics on the exposed coating binder phase. The build-up of this intermetallic diffusion barrier dramatically reduces the rate of counter-current Co and

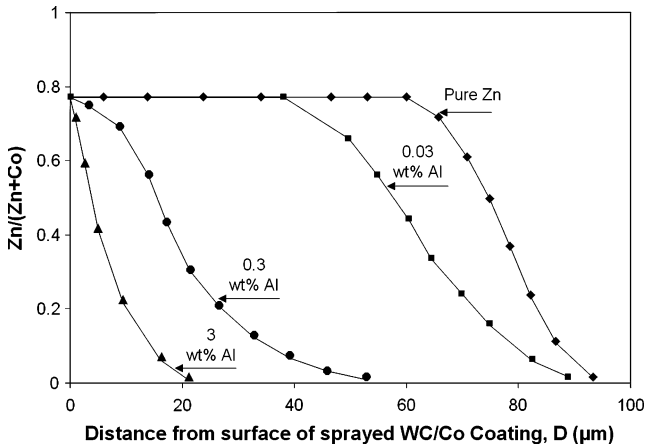

Fig. 3 Effect of the bath Al concentration on the Zn and Co concentration profiles in the diffusion layer of WC-Co thermal spray coatings after immersion at 480 °C for 168 h. Redrawn from Ref 43

Zn diffusion and hence the rate of coating degradation relative to that in pure Zn (Ref 43).

Seong et al. have noted that the level of W dissolved in the Co binder plays an important role in the Co reactivity with Al in the bath (Ref 31). In pure Zn, higher W contents generate higher reaction rates of the Co binder. It is postulated that W destabilizes the Co-Zn intermetallic phase, disrupting the formation of a continuous Co-Zn surface layer (Ref 31). Conversely, the reduction in Co reactivity with Al at higher W contents (20-30 wt.%) is thought to result from the stabilizing effect of W on the interface between the surface Co-Al intermetallic compounds and the underlying Co binder phase (Ref 31). The build-up of a stable Co-Al layer increases the diffusion barrier for attack of the binder, thereby reducing the coating corrosion rate.

Seong et al. (Ref 28) have shown that the effectiveness of this generic reaction mechanism varies as a function of industrial conditions in their study of WC-12 wt.% Co Jet Kote HVOF coatings on pot rolls in galvanizing baths of 0.12-0.23 wt.% Al. The mid-span of the roll in continuous contact with the steel sheet for 33 days showed minimal degradation and a Zn diffusion depth of 10 μm. A complex layer structure of reaction products formed with extended exposure out to 56 days. Zn and Al had diffused to depths of 20 μm in the coating. Above this a dense layer of Co-Al intermetallics formed, some of which had reacted further to Fe_2Al_5. The inclusion of WC-Co particles within this layer indicated that preferential molten metal attack occurred along the coating splat boundaries. On top of this, a thick Zn- and Al-rich reaction layer formed containing ZnO particles. The higher Al concentration evident in the corrosion products was surprising given that the Al-content of the bath was <0.23 wt.%.

In contrast, areas of the roll not in continuous contact with the steel sheet showed Zn and Al diffusion depths of 40 μm, but no Al or Fe rich reaction products on the coating surface. This variation in corrosion rate with degree of wear highlights the synergy of corrosion and

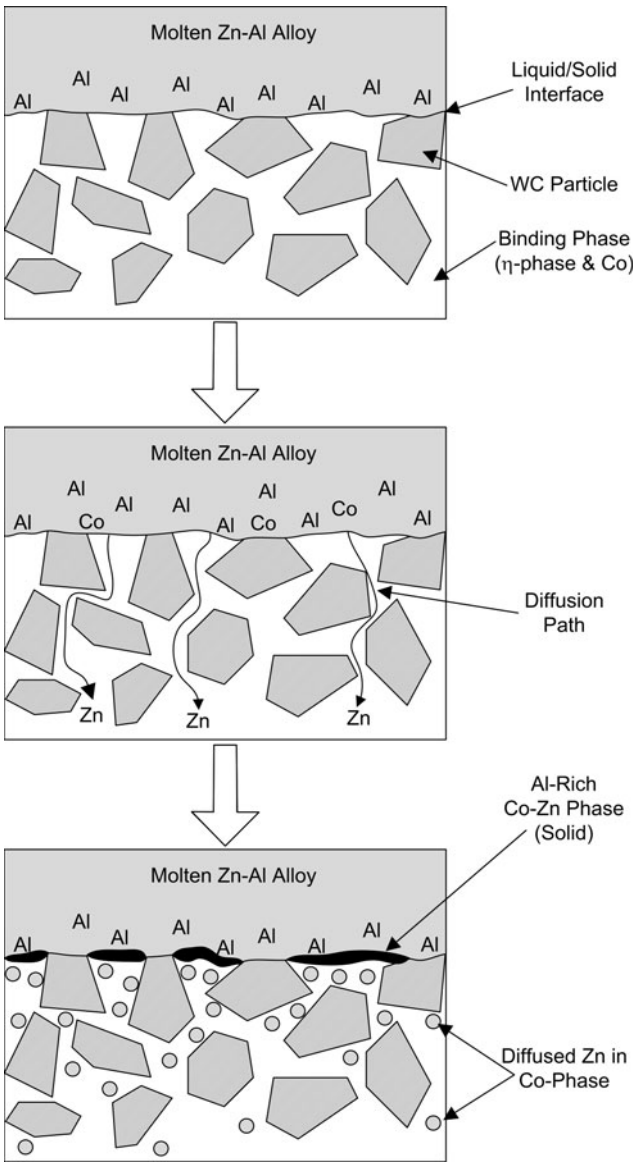

Fig. 4 Schematic diagram illustrating the diffusion mechanisms within WC-Co coatings immersed in Zn-Al baths. Schematic redrawn based on Ref 43

wear in accelerating the attack of the alloy and the occurrence of a potentially more complex degradation mechanism.

Away from contact with the sheet, cracking of the WC-Co coating allowed penetration of the Zn-Al bath. Co-Al was the dominant reaction product, in spite of the low bath Al concentration, and Al diffused significantly further that Zn from the cracks into the coating in direct contrast with the lab tests of Tani et al. (Ref 43).

At higher Al-contents characteristic of galvalume conditions, WC-Co coatings undergo severe dissolution of the Co phase. In the work of Tan et al. (Ref 44) attack of the matrix phase in JP-8000 sprayed WC-Co coatings was readily evident after 24 h exposure and continued to increase in severity with continued exposure.

3.1.3 Cr Additions to the WC-Co Binder. Additions of 2-9 wt.% Cr are added to the WC-Co binder to enable the formation of a protective Cr_2O_3 oxide layer on the binder phase to extend the lifetime of the coating (Ref 40). Similar effects have been observed for bulk 316 stainless steel (Ref 8), where the adherent Cr_2O_3 oxide is not well wetted by Zn-Al melts and therefore acts to protect the steel. By preventing corrosion, the oxide also prevents the formation of Fe_2Al_5 to which dross particles adhere and hence minimizes dross pick-up on the surface of the bath hardware. Unfortunately, this beneficial effect is short lived due to oxide dissolution and cracking which degrade the oxide layer integrity and allows attack of the substrate (Ref 8).

3.1.4 Cracking of WC-Co Thermal Spray Coatings. The rapid liquid metal attack of the coating and underlying substrate that occurs through cracking of the coating necessitates particular attention during the coating production process and during subsequent handling and installation. Cracks may be generated as a result of various mechanisms:

- Build-up of residual stresses during thermal spraying (Ref 10).
- Stress generation resulting from the variation in the coefficient of thermal expansion between the coating and the pot roll material (Ref 10, 27, 40).
- Mechanical loading and impact on the roll in-service (Ref 10, 27).

Thermal expansion induced cracking is controlled through selection of the pot roll material and the WC-Co coating thickness. 316 Stainless Steel is the most commonly used pot roll material, but its high coefficient of thermal expansion makes WC-Co coatings on its surface prone to cracking and spallation (Ref 10). This mechanism was postulated to account for the superior Zn corrosion resistance of plasma-sprayed WC-Co coatings on carbon steel substrates relative to the same coating on 316 Stainless Steel substrates in Ref 25. Similarly, the lower thermal expansion of 400 series stainless steels has enhanced their application as substrate materials for WC-Co coatings under industrial conditions (Ref 10).

The results of trials discussed in Ref 7 in which 100 μm WC-Co coatings on 316 Stainless Steel did not crack in molten Zn, while 150 μm coatings spalled, indicate the critical role of the coating thickness in the overall coating ductility. Mizuno and Kitamura have formulated a relationship between the thermal expansion properties of the coating and substrate, and the coating porosity to determine acceptable limits on the coating thickness for molten metal applications (Ref 45). They specify the following (Eq 2):

$$C_d = \alpha_1/(t * \alpha_2), \quad \text{(Eq 2)}$$

where α_1 is coefficient of thermal expansion of the thermal spray coating, α_2 is coefficient of thermal expansion of the base material or underlying bond coating, and t is coating thickness (μm).

To prevent cracking and spallation, it is preferable that $C_d \geq 0.15 \times 10^{-2}$. For a given coating-substrate pair, C_d is maximized by using the thinnest coating possible. However, as the coating thickness decreases, the likelihood increases of ''through-holes'' directly connecting the molten metal to the substrate via interconnected porosity (Ref 40, 45). The following boundary condition on the coating thickness is therefore proposed, where P is the coating porosity (%) (Eq 3). For this condition, the porosity must not exceed 10%, and preferably be <4%.

$$t - 23e^{0.3P} \geq 0. \quad \text{(Eq 3)}$$

As a final measure, particular care must be exercised during handling and installation of coated pot rolls in the galvanizing bath. Any mechanical impact on the coated surface risks cracking the coating (Ref 10). Similarly, a pre-heating process should also be implemented prior to installation to prevent cracking and spallation from thermal shock (Ref 10, 29).

3.1.5 Sealants. Sealants are commonly applied to thermal spray WC-Co coatings to reduce molten metal ingress through open porosity. However, the high velocity thermal spray methods typically used to deposit WC-Co powders generate low degrees of coating porosity, minimizing the penetration of fluid sealants to the near surface region (Ref 10). Seong et al. (Ref 10) applied a chromic acid treatment to seal WC-12 wt.% Co Jet Kote HVOF coatings with Cr_2O_3 for pot rolls in an industrial galvanizing bath. The Cr_2O_3 layer prevented direct contact of the molten Zn-Al with the coating, but did not prevent Zn and Al from diffusing up to 40 μm into the coating after 56 days in-service. However, it was unclear to what degree these diffusing elements reacted to form intermetallic phases within the coating or their effect on the coating integrity.

Mizunuma et al. (Ref 46) have developed an innovative sealing process that goes beyond the conventional ''apply sealant solution/slurry and dry'' method by exploiting the reactivity of WB with chromic acid treatment. WB oxidizes to form volatile B_2O_3, but retains a layer of this oxide on the surface. When a concentrated chromic acid solution is applied and heated, the acid is converted to CrO_3. Above 200 °C, CrO_3 melts and eventually oxidizes further to Cr_2O_3 at 400 °C. During this process, vitrification of B_2O_3 occurs at 300 °C. The vitrified B_2O_3 reacts with the molten CrO_3 to form a CrO_3-B_2O_3 glass phase, which reacts further to form a Cr_2O_3-B_2O_3 glass phase above 400 °C. This fluid phase effectively seals any cracks and pores within the coating. WC-Co HVOF coatings incorporating a percentage of WB and treated with chromic acid lasted three times as long (30 days versus 10 days) as WC-10 wt.% Co and WC-12 wt.% Co-5 wt.% Cr HVOF coatings sealed with chromic acid treatment during immersion in Zn-3%Al at 500 °C (Ref 46).

3.2 Oxide-Based Thermal Spray Coatings

3.2.1 Graded Coatings. Oxide ceramics offer the benefit of a high melting point, high hardness and wear resistance, and chemical stability at high temperature in molten metal environments (Ref 26, 47-49). Many oxides, particularly Al_2O_3 and yttria-stabilized zirconia (Ref 26) are not wetted by liquid zinc and are therefore particularly resistant to corrosion. Such properties make oxide-based coatings particularly attractive for high temperature, high Al-content, and galvalume baths where the more common WC-Co-based coatings do not perform well (Ref 27).

The complex stress-state formed during rapid solidification of molten ceramic droplets during thermal spraying generates residual tensile stresses which limit the maximum coating thickness. Thermal cycling and the variation in thermal expansion between the oxide coating and metallic substrate compound the tensile stress state, making the coating prone to spallation (Ref 26, 27, 50). Gradient coatings are traditionally employed to accommodate this complex stress state by continually varying the ratio of ceramic-to-metallic material from metallic-rich at the substrate surface to ceramic-rich at the coating surface. The composition gradient reduces stress formation during spraying and coefficient of thermal expansion mismatch with the substrate, allowing thicker coatings to be formed (Ref 47). The effectiveness of this concept is illustrated in the work of Dong et al. (Ref 47) where a plasma-sprayed NiAl-ZrO_2 gradient coating lasted three times as long as a conventional ZrO_2 plasma-sprayed coating of comparable thickness in molten Zn. In the conventional coating, microcracks, pores, and splat boundaries provided paths for molten metal penetration (Ref 26, 41, 47-49). Corrosion of the bond coat and substrate by the Zn-Al melt led to selective dissolution and intermetallic formation. The volume expansion of the corrosion products generated flaking and spallation of the coating, typically evident as circular flakes of 3-5 mm diameter (Ref 41). The coating therefore acted as a purely nonreacting physical barrier to Zn penetration, with its effectiveness dictated by the physical defect density of the coating microstructure.

Failure of the graded coating occurred by diffusion of Zn through the outer ZrO_2 layer followed by dissolution and reaction of the NiAl binder (Ref 47). In this way, ceramic-based composites tend to be limited not by the composite coating microstructure, but instead by the Zn corrosion resistance of the binder phase.

The longevity of thermal spray coatings with a conventional splat-based microstructure can be improved through the use of sealing compounds such as hexagonal boron nitride in a binder, graphite in a binder, thermally sprayed chromium oxide, hydrated chromium oxide, porcelain, and molybdenum disulfide (Ref 27). These compounds seal microcracks and pores which are typically more prevalent in ceramic thermal spray coatings relative to high velocity sprayed WC-Co coatings. Cr_2O_3-based sealants are limited to galvanizing baths of low Al concentration. Cr_2O_3 is reduced by Al in the melt, resulting in dissolution of this phase (Ref 48). Break down of the sealed surface layer with extended exposure typically occurs by stress-induced cracking. Hence, such measures act to delay rather than prevent coating breakdown by liquid zinc.

3.2.2 Multilayer Coatings. The use of multilayered coatings (Ref 27, 29, 41, 51) is aimed at exploiting the advantages of a particular coating composition while compensating for its limitations through the use of additional subcoatings. This concept is illustrated in the patent of Nitta and Tsuyuki (Ref 41) who developed a three-layer thermal spray coating stack for continuous hot-dip galvanizing pot rolls:

- *Base layer*: High Co-content alloy or cermet with high Co-alloy content.
- *Middle layer*: Mo cermet containing oxide, carbide or boride phases.
- *Top layer*: Oxide ceramic coating.

The Ni-Co-Cr alloy-based base layer formed a high density coating largely free of cracks and pores. The composition was resistant to molten Zn-Al alloy attack. Where reaction did occur due to Zn diffusion through the more porous ceramic top layer, it was postulated that the intermetallic phases formed acted to seal any pores in the coating.

The intermediate Mo cermet layer performed two functions. The hardness of this layer reduced deformation of the coating stack under the external loads imposed by the steel sheet passing around the roll. This minimized the strain on the ceramic top layer and reduced the risk of cracking/spallation. In addition, the cermet layer had a coefficient of thermal expansion intermediate between the substrate and Co-alloy material below and the ceramic coating above. The transition in thermal expansion properties reduced the mismatch between coating layers and therefore further reduced the risk of cracking and spallation. The ceramic top coat exploited the low wettability and reactivity of partially stabilized ZrO_2 to extend the operating lifetime of the coated component in-service.

In service, a pot roll coated in this manner lasted 120 days before showing signs of localized flaking on the surface. In contrast, a comparison trial using a ZrO_2 oxide + cermet coating stack lasted only 24 days before developing 3 mm circular flakes on the surface (Ref 41).

3.2.3 Substrate Protection. Localized breakdown of the ceramic coating on pot rolls forms corrosion pits in the substrate and results in localized spallation of the ceramic top coat. While the ceramic degradation remains small, it does not significantly reduce the surface quality of the galvanized sheet and hence may remain for an extended period in-service. However, by the time the ceramic spallation is sufficient to require maintenance of the roll, extensive corrosion of the substrate occurs, requiring significant machining of the substrate to a depth below the corrosion pits (Ref 52). This significantly reduces the number of cycles that the roll can be refurbished and recoated before the diameter becomes too small. To combat this, Betts (Ref 52) has proposed the inclusion of a thin (<175 μm) corrosion-resistant layer of Mo- or W-based alloy beneath the metallic bond coat. This limits Zn corrosion to the layers above. Minimal, if any, machining of the roll material itself is required during maintenance and the lifetime of the roll is therefore significantly extended (Ref 52). No other reference has been found to the use of this unique Mo/W base coating, and as such its effectiveness versus more conventional multilayered coatings has yet to be quantified in the open literature.

3.3 Boron Containing Thermal Spray Coatings

The improved corrosion resistance of Al-Zn over Zn-coated steel sheet has significantly increased its use in the auto and consumer product industries (Ref 44). The poor performance of conventional WC-Co coatings in the highly corrosive, high temperature Al-Zn-Si galvalume baths (Ref 37, 39, 53) has led to the recent development of corrosion-resistant boride containing coatings (Ref 26, 37-39, 44, 45, 51, 53-59). Fujimi Incorporated (Japan) (Ref 59) has developed a new MoB/CoCr HVOF coating for galvalume baths which has shown dramatically longer operating lifetimes relative to conventional optimized WC-Co and WC-Co-Cr HVOF coatings (Ref 37-39 and Fig. 5).

The desired cermet composition consists of 40-50 wt.% Mo, 6-10 wt.% B, 20-35 wt.% Co, and 15-20 wt.% Cr with up to 5 wt.% of additional elements (Ref 59). Powder sintering during production is critical to the formation of complex Co-Mo-B, Cr-Mo-B, and Co-Cr-Mo-B phases which account for the Al-Zn-Si corrosion resistance in a similar manner to the complex Co-W-C phases in WC-Co coating in Zn-Al melts. In this way, the concentration of the free metallic Co, which is prone to rapid reaction with the molten metal, is minimized. After thermal spraying,

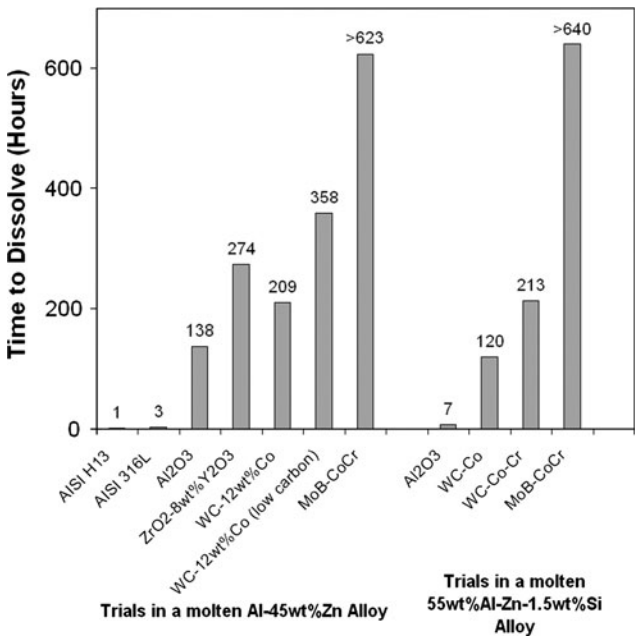

Fig. 5 Lifetime of thermal spray coatings of different composition in molten alloys of Al-45 wt.% Zn (*left*) and 55 wt.% Al-Zn-1.5 wt.% Si (*right*). Data redrawn from Ref 37 and 39

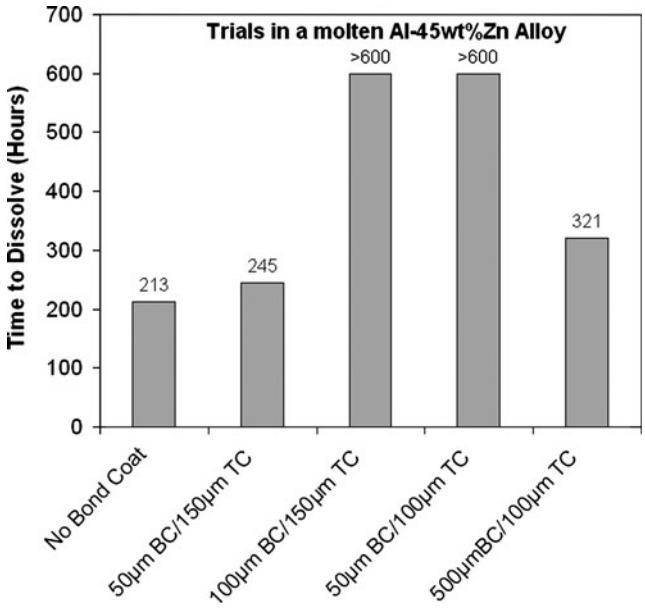

Fig. 6 Lifetime of thermally sprayed samples immersed in a molten Al-45 wt.% Zn alloy. The two-layered coating consisted of a Co-30 wt.% Cr-4 wt.% W-1.2 wt.% C bond coat (BC) and a MoB/CoCr top coat (TC) of varying thicknesses and sprayed onto a AISI 316L Stainless Steel substrate. Data redrawn from Ref 39

the primary coating phases are $CoMo_2B_2$ and CoMoB (Ref 37-39) with the Cr content presumably alloyed into the complex Co binder phase (Ref 39).

Coatings immersed in laboratory 55% Al-Zn-1.5% Si galvalume baths at 657-710 °C for up to 640 h showed no signs of thickness reduction, dissolution of coating phases, or internal diffusion of Al or Zn into the coating (Ref 37, 38, 44). However, the coatings were observed to spall from the substrate at the conclusion of testing due to thermal expansion mismatch (Ref 37). While the coefficient of thermal expansion of MoB/CoCr coatings is larger than WC-Co coatings (9.2×10^{-6} versus $6.8\text{-}7.2 \times 10^{-6}$, Ref 39), thermal expansion mismatch is still the life-limiting factor for this coating (Ref 39). Mizuno and Kitamura cyclically tested several combinations of JP-5000 HVOF sprayed Co-30 wt.% Cr-4 wt.% W-1.2 wt.% C bond coat and MoB/CoCr top coat thickness's on 316L Stainless Steel substrates to determine the coating lifetime under galvalume conditions (Fig. 6). The combination of thin (50 μm) bond coat and thick (150 μm) MoB-CoCr top coat underwent significant cracking and delamination within the top coat layer. Conversely, the combination of very thick bond coat (500 μm) and thin (100 μm) MoB-CoCr top coat failed due to spallation of the bond coat from the substrate. The greatest lifetimes (>600 h) were achieved with bond coat/MoB-CoCr top coat combinations of 100/150 μm and 50/100 μm.

Of significance was the variation in thermal expansion with temperature as a function of heat treatment for the thermally sprayed bond coat and MoB-CoCr top coat (Ref 39). Both coatings showed high initial expansion ratios, which became smaller and more stable after multiple heating/cooling cycles. Recrystallization of the amorphous as-sprayed structure and relaxation of residual stresses were postulated to account for this response highlighting that appropriate pretreatment is necessary prior to use in industrial applications (Ref 39).

4. Summary

Sheet steel destined for outdoor use is typically coated with Zn-based alloys in a continuous hot-dip process to improve its corrosion resistance. The molten zinc environment is very corrosive to the traditional Fe- and Co-based alloys used to build bath hardware. Three thermal spray coating solutions are now routinely used to improve the corrosion resistance of the bath components.

4.1 WC-(10-15 wt.%)Co Coatings

- Resistance to corrosion in molten Zn-based alloys relies on the formation of complex Co-W-C phases formed by reaction between WC and Co during powder preparation and thermal spraying. This effect can be enhanced through reductions in the WC-Co carbon content and the use of finer starting carbide grains.
- Cr additions to the Co binder enable the formation of a protective Cr_2O_3 layer that is not wetted by Zn-Al melts and prevents "dross" pick-up. However, such beneficial effects are short lived.

4.2 Oxide-Based Coatings

- Oxide-based coatings are attractive for high Al-content galvalume baths where WC-Co coatings do not perform as well as in galvanizing baths. However, the complex stress-state formed during spraying limits the maximum coating thickness.
- Continuously graded coatings accommodate the complex stress state, but their effectiveness is dictated by the corrosion resistance of the metallic binder.
- An alternative solution is the use of multilayered coatings comprised of a ceramic top coat, an oxide-based cermet middle layer and a Co-alloy-based bond coat. The optimized composition and microstructure of each layer greatly extend the operating lifetime of galvanizing hardware relative to conventional two-layered oxide top coat/metallic bond coat coatings.

4.3 Boron-Containing Coatings

- Recent developments in MoB/CoCr coatings have shown dramatic improvements in corrosion resistance relative to conventional WC-Co and WC-Co-Cr coatings in high Al-content galvalume baths.

- The corrosion resistance is attributed to the formation of complex Co-Cr-Mo-B phases.
- The thermal expansion properties require tailoring of the appropriate bond coat and top coat thicknesses to generate the longest coating lifetimes.

The thermal spray industry is undergoing dramatic scientific and industrial advances in order to keep pace with the demands of modern industry. This is reflected in the development of tailored WC-Co coatings for galvanizing baths and the recent developments of corrosion-resistant MoB-based coatings to cater for the increasing demand for galvalume coatings. As industry awareness and acceptance of this technology continue to develop, new and improved coating solutions will be increasingly incorporated. These are expected to improve the performance of current steel making practice while enabling significant advancements in the next generation of equipment through improved surface functionality, durability, and reliability.

References

1. H.E. Townsend, Continuous Hot Dip Coatings, *ASM Handbook Volume 5: Surface Engineering*, Vol 5, ASM International, 1994, p 339-348
2. A.R. Marder, The Metallurgy of Zinc-Coated Steel, *Prog. Mater. Sci.*, 2000, **45**, p 191-271
3. GalvInfoNote 2.4—The Role of Aluminium in Continuous Hot-Dip Galvanizing (Revision 1.1 March 2009), Retrieved 9 February 2010 from GalvInfo Centre Web site: http://www.galvinfo.com/
4. The Science of Steel, Retrieved 3 February 2010 from the NZ Steel Web site: http://www.nzsteel.co.nz/go/about-new-zealand-steel/student-information/the-science-of-steel
5. M. Bright and A. Ensminger, Identification of Failure Mechanisms in Correcting Roll Bearings of a Continuous Galvanizing Line, *2004 Galvanizers Association Annual Meeting*, Charleston, South Carolina, USA, 2004
6. K. Zhang and L. Battiston, Sliding Wear of Various Materials in Molten Zinc, *Mater. Sci.Technol.*, 2002, **18**, p 1551-1560
7. E. Barbero and C. Irwin, *Development of Improved Materials for Continuous Steel Hot-Dipping Processes—Final Technical Report (DOE Project Award Number: DE-FC36-01ID14042)*, West Virginia University, USA, 2005
8. K. Zhang, N.Y. Tang, F.E. Goodwin, and S. Sexton, Reaction of 316L Stainless Steel With a Galvanizing Bath, *J. Mater. Sci.*, 2007, **42**, p 9736-9745
9. J. Morando, Material Formulation for Galvanizing Equipment Submerged in Molten Aluminium and Aluminium/Zinc Melts, United States Patent, Publication Number US6168757 B1. Alphatech Inc., 2001
10. B.G. Seong, S.Y. Hwang, M.C. Kim, and K.Y. Kim, Reaction of WC-Co Coatings with Molten Zinc in a Zinc Pot of a Continuous Galvanizing Line, *Surf. Coat. Technol.*, 2001, **138**, p 101-110
11. X. Liu, V. Sikka, M. Bright, S. Sexton, E. Barbero, and J. Hales, Development of a New Weld Overlay for Pot Hardware in Continuous Galvanizing Lines, *GALVATECH 07—7th International Conference on Zinc and Zinc Alloy Coated Steel Sheet*, Osaka, Japan, 2007
12. H. Kim, B. Yoon, and C. Lee, Sliding Wear Performance in Molten Zn-Al Bath of Cobalt-Based Overlayers Produced by Plasma Transferred Arc Weld-Surfacing, *Wear*, 2003, **254**, p 408-414
13. M. Bright, Investigating Galvanneal Reactions on Pot Hardware Materials, *AISTech 2007 Conference*, Indianapolis, USA, 2007
14. X. Liu, E. Barbero, J. Xu, M. Burris, K. Chang, and V. Sikka, Liquid Metal Corrosion of 316L, Fe_3Al, and FeCrSi in Molten Zn-Al Baths, *Metall. Mater. Trans. A*, 2005, **36A**, p 2049-2058
15. J. Xu, M. Bright, X. Liu, and E. Barbero, Liquid Metal Corrosion of 316L Stainless Steel, 410 Stainless Steel, and 1015 Carbon Steel in a Molten Zinc Bath, *Metall. Mater. Trans. A*, 2007, **38A**, p 2727-2736
16. J. Xu, X. Liu, M. Bright, J. Hemrick, V. Sikka, and E. Barbero, Reactive Wetting of an Iron-Base Superalloy MSA2020 and 316L Stainless Steel by Molten Zinc-Aluminium Alloy, *Metall. Mater. Trans. A*, 2008, **39A**, p 1382-1391
17. E. Baril and G. L'Esperance, Studies of the Morphology of the Al-Rich interfacial Layer Formed During the Hot Dip Galvanizing of Steel Sheet, *Metall. Mater. Trans. A*, 1999, **30A**, p 681-695
18. M. Bright and E. Barbero, Effect of Aluminium Concentration of the Dissolution of 316L Stainless Steel in Molten Zinc, *7th International Conference on Zinc and Zinc Alloy Coated Steel Sheet*, Osaka, Japan, 2007, p 94-99
19. K. Zhang and N. Tang, Reactions of Co Based and Fe Based Superalloys With a Molten Zn-Al Alloy, *Mater. Sci. Technol.*, 2004, **20**, p 476-739
20. D. Yan, J. He, B. Tian, Y. Dong, X. Li, J. Zhang, L. Xiao, and W. Jing, The Corrosion Behaviour of Plasma Sprayed Fe_2Al_5 Coating in Molten Zn, *Surf. Coat. Technol.*, 2006, **201**, p 2662-2666
21. W.J. Wang, J.P. Lin, Y.L. Wang, and G.L. Chen, The Corrosion of Intermetallic Alloys in Liquid Zinc, *J. Alloy Compd.*, 2007, **428**(1-2), p 237-243
22. J. Song and H. Kim, Sliding Wear Performance of Cobalt Based Alloys in Molten Al Added Zinc Bath, *Wear*, 1997, **210**, p 291-298
23. M.X. Yao, J.B.C. Wu, and R. Liu, Microstructural Characteristics and Corrosion Resistance in Molten Zn-Al Bath of Co-Mo-Cr-Si Alloys, *Mater. Sci. Eng. A*, 2005, **407**, p 299-305
24. W. Xibao, Corrosion of Co-Cr-W Alloy in Liquid Zinc, *Metall. Mater. Trans. A*, 2003, **34B**, p 881-886
25. M. Bright, "Dissolution and Diffusion Characteristics of 316L Stainless Steel in Molten Zinc Containing Variable Concentrations of Aluminium," Doctoral Thesis, College of Engineering and Mineral Resources, West Virginia University, Morgantown, West Virginia, 2007
26. X. Ren, X. Mei, J. She, and J. Ma, Materials Resistance to Liquid Zinc Corrosion on Surface of Sink Roll, *Proceedings of Sino-Swedish Structural Materials Symposium 2007*, 2007, p 130-136
27. H.H. Fukubayashi, Present Furnace and Pot Roll Coatings and Future Development, *Proceedings of the International Thermal Spray Conference 2004*, 10-12 May, 2004 (Osaka, Japan), ASM International, 2004, p 125-131
28. B.G. Seong, S.Y. Hwang, M.C. Kim, K.Y. Kim, Observation on the WC-Co Coating Used in a Zinc Pot of a Continuous Galvanizing Line, *Thermal Spray: Surface Engineering Via Applied Research*, C.C. Berndt, Ed., 8-11 May, 2000 (Montréal, QC, Canada), ASM International, Materials Park, OH, USA, 2000, p 1159-1167
29. M. Sawa and J. Oohori, Application of Thermal Spraying Technology at Steelworks, *Thermal Spraying: Current Status and Future Trends—Proceedings of the 14th International Thermal Spray Conference*, A. Ohmori, Ed., May 22-26, 1995 (Kobe, Japan), High Temperature Society of Japan, 1995, p 37-42
30. R.L. Hao, Thermal Spraying Technology and Its Applications in the Iron & Steel Industry in China, *Thermal Spray 2007: Global Coating Solutions*, B.R. Marple, M.M. Hyland, Y.C. Lau, C.J. Li, R.S. Lima and G. Montavon, Ed., 14-16 May, 2007 (Beijing, China), ASM International, Materials Park, OH, USA, 2007, p 291-296
31. B.G. Seong, S.Y. Hwang, and K.Y. Kim, Factors on the Corrosion Resistance of Thermally Sprayed WC-Co Coatings in Molten Zinc, *Proceedings of the 1st International Surface Engineering Congress*, 2003, p 555-562
32. Y. Harada and K. Tani, Spray-Coated Roll for Continuous Galvanization, United States Patent, Publication Number US 5316859. Tocalo Co. Ltd., 1994
33. L. Jacobs, *Structure-Property Relations and Decarburisation in WC-Cermet Coatings Deposited by High Velocity (HV) Thermal Spray Techniques*, Department of Chemical and Materials

Engineering, Auckland, New Zealand, University of Auckland, 1999, p 226
34. L. Jacobs, M.M. Hyland, and M.d. Bonte, Comparative Study of WC-Cermet Coatings Sprayed Via the HVOF and HVAF Processes, *J. Therm. Spray Tech.*, 1998, **7**(2), p 213-218
35. L. Jacobs, M.M. Hyland, and M.d. Bonte, Study of the Influence of Microstructural Properties on the Sliding-Wear Behaviour of HVOF and HVAF Sprayed WC-Cermet Coatings, *J. Therm. Spray Tech.*, 1999, **8**(1), p 125-132
36. T. Tomita, Y. Takatani, Y. Kobayashi, Y. Harada, and H. Nakahira, Durability of WC/Co Sprayed Coatings in Molten Pure Zinc, *ISIJ Int.*, 1993, **33**(9), p 982-988
37. H.P. Lv, J. Wang, C.S. Zhai, F. Li, B.D. Sun, Durability of HVOF Sprayed MoB/CoCr Coating on the 316L Stainless Substrate in Molten 55%Al-Zn-1.5%Si Bath, *Thermal Spray 2007: Global Coating Solutions*, B.R. Marple, M.M. Hyland, Y.C. Lau, C.J. Li, R.S. Lima, and G. Montavon, Ed., 14-16 May, 2007 (Beijing, China), ASM International, Materials Park, OH, USA, 2007, p 513-517
38. H. Mizuno, J. Kitamura, S. Osawa, and T. Itsukaichi, Development of Durable Spray Coatings in Molten Aluminum Alloy, *Proceedings of the 2005 International Thermal Spray Conference*, E. Lugscheider, Ed., 2-4 May, 2005 (Basel, Switzerland), ASM International, Materials Park, OH, USA, 2005
39. H. Mizuno and J. Kitamura, MoB/CoCr Cermet Coatings by HVOF Spraying Against Erosion by Molten Al-Zn Alloy, *J. Therm. Spray Tech.*, 2007, **16**(3), p 404-413
40. W. Jarosinski, J. Quest, D. Wang, V. Belov, and S.A. Kleyman, Thermal Spray Coated Rolls, World Patent, Publication Number WO2007047330 (A1). Praxair Technology Inc, 2007
41. H. Nitta and A. Tsuyuki, Pot Roll for Continuous Hot-Dip Galvanizing, European Patent, Publication Number EP 0712939 A2. Praxair S.T. Technology Inc., 1996
42. SINM Coatings Service, Retrieved 3 February 2010 from the Inframat Website: http://www.inframat.com/steel.htm
43. K. Tani, T. Tomita, Y. Kobayashi, Y. Takatani, and Y. Harada, Durability of Sprayed WC/Co Coatings in Al-Added Zinc Bath, *ISIJ Int.*, 1994, **34**(10), p 822-828
44. X.H. Tan, Z.H. Jiang, Y.G. Zhang, J.S. Sun, Investigation of the Corrosion Behaviour of HVOF-Sprayed Carbide Cermet Coatings in Molten Al-Zn-Si Alloy Bath, *Thermal Spray 2007: Global Coating Solutions*, B.R. Marple, M.M. Hyland, Y.C. Lau, C.J. Li, R.S. Lima, and G. Montavon, Ed., 14-16 May, 2007 (Beijing, China), ASM International, Materials Park, OH, USA, 2007, p 937-942
45. H. Mizuno and J. Kitamura, Thermal Spray Coating and Thermal Spray Powder, United States Patent, Publication Number US 2007/0184253. 2007
46. M. Mizunuma, T. Uchiyama, and K. Tarumi, Method of Manufacturing an Immersion Member with Pore-Sealing Layer, United States Patent, Publication Number US 5395661. Nippon Steel Hardfacing Co Ltd., 1995
47. Y. Dong, D. Yan, J. He, J. Zhang, and X. Li, Degradation Behaviour of ZrO_2-Ni/Al Gradient Coatings in Molten Zn, *Surf. Coat. Technol.*, 2006, **201**, p 2455-2459
48. T. Sato, K. Tarumi, Y. Michikata, Y. Horie, and J. Yasuoka, Member With Film Formed by Thermal Spraying of Thermal Spray Material, United States Patent, Publication Number US 6569546. Nippon Steel Hardfacing Co. Ltd., 2003
49. K. Hollis, M. Peters, and B. Bartram, Plasma-Sprayed Ceramic coatings for Molten Metal Environments, *Thermal Spray 2003: Advancing the Science and Applying the Technology*, C. Moreau and B. Marple, Ed., 5-8 May, 2003 (Orlando, FL), ASM International, Materials Park, OH, USA, 2003, p 153-158
50. N. Noda, M. Yamada, Y. Sano, S. Sugiyama, and S. Kobayashi, Thermal Stress for All-Ceramic Rolls Used in Molten Metal to Produce Stable High Quality Galvanized Steel Sheet, *Eng. Fail. Anal.*, 2008, **15**, p 261-274
51. S.Y. Hwang and B.G. Sung, Method for Coating Oxides on Roll Used in Hot Dip Galvanizing Pot, Korean Patent, Publication Number KR 20020051089. Posco Res. Inst. Science and Tech., 2002
52. R. Betts, Refractory Metal Coated Articles for Use in Molten Metal Environments, United States Patent, Publication Number US 6534196. Cincinnati Thermal Spray, 2003
53. H. Mizuno, S. Tawada, I. Aoki, and J. Kitamura, HVOF Coatings of MoB/CoCr Against Erosion by Molten Al-Zn Alloy, *Thermal Spray 2007: Global Coating Solutions*, B.R. Marple, M.M. Hyland, Y.C. Lau, C.J. Li, R.S. Lima, and G. Montavon, Ed., 14-16 May, 2007 (Beijing, China), ASM International, Materials Park, OH, USA, 2007, p 567-571
54. Y. Harada, T. Oka, and J. Takeuchi, Member for Molten Metal and its Production, Japanese Patent, Publication Number JP 2236266. Tocalo Co. Ltd., 1990
55. Y. Kurisu and K. Ando, Member for Hot Dip Metal Bath and Its Production, Japanese Patent, Publication Number JP 11061369. Nippon Steel Corp., 1999
56. Y. Harada, K. Tani, and T. Doi, Composite Film Coated Member Excellent in Wear Resistance and Molten Metal Resistance and its Manufacture, Japanese Patent, Publication Number JP 4088159. Tocalo Co. Ltd., 1992
57. H.P. Lv, J. Wang, C.S. Zhai, F. Li, and B.D. Sun, Study of Microstructure, Vickers Microindentation and Microhardness Distribution of HVOF Sprayed Composite MoB/CoCr Coating, *Thermal Spray 2007: Global Coating Solutions*, B.R. Marple, M.M. Hyland, Y.C. Lau, C.J. Li, R.S. Lima, and G. Montavon, Ed., 14-16 May, 2007 (Beijing, China), ASM International, Materials Park, OH, USA, 2007, p 528-532
58. J. Wood, S. Katoh, and H. Nitta, Molten Zinc Resistant Alloy and Its Manufacturing Method, United States Patent, Publication Number US 5456950. Praxair S.T. Technology Inc., 1995
59. T. Itsukaichi and S. Osawa, Thermal Spraying Powder and Method of Forming a Thermal Sprayed Coating Using the Same, United States Patent, Publication Number US 6984255 B2. Fujimi Inc., 2006